

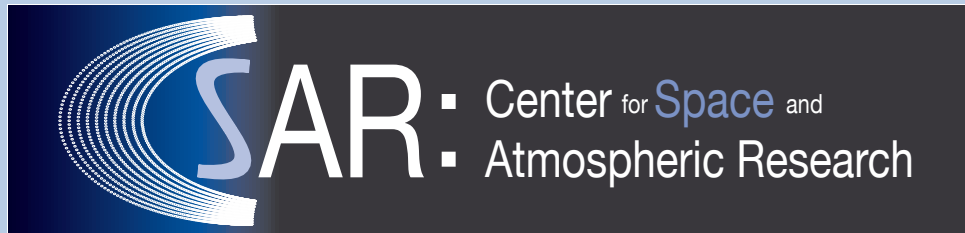
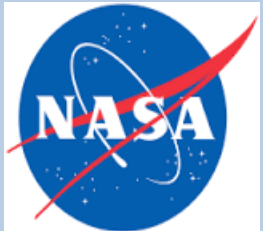
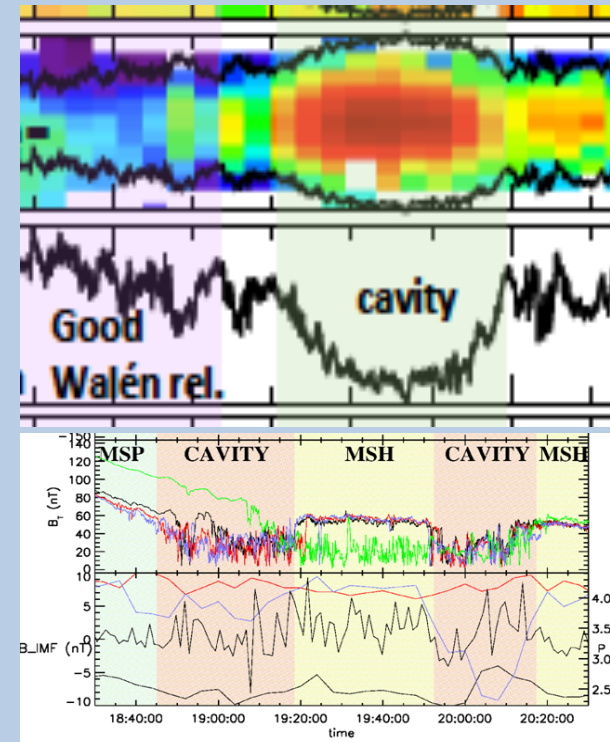
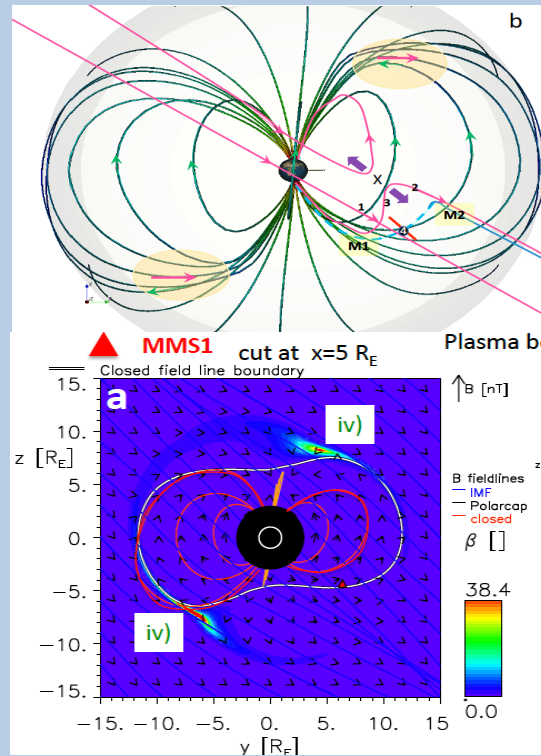
# Diamagnetic Cavities - High-Latitude, Dayside Source of Energetic Particles in the Earth's Magnetosphere.

Katariina Nykyri, Embry-Riddle Aeronautical University

## Motivation:

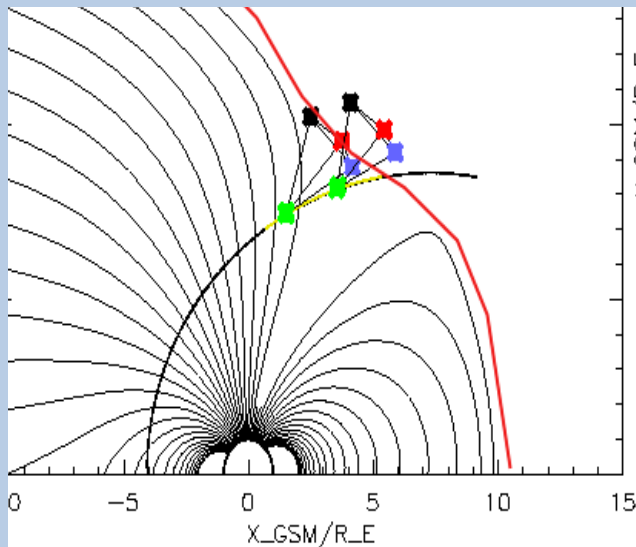
- How much mass do dayside diamagnetic cavities contain?
- Can the 100s of keV energetic particles in the cavities provide portion of the seed population for radiation belts?
- What are the detailed physical mechanisms allowing transport of these particles deeper to the inner magnetosphere?

Studies presented were/are supported by NSF grant #0847120 and NASA grants #NNX17AI50G #80NSSC18K1381

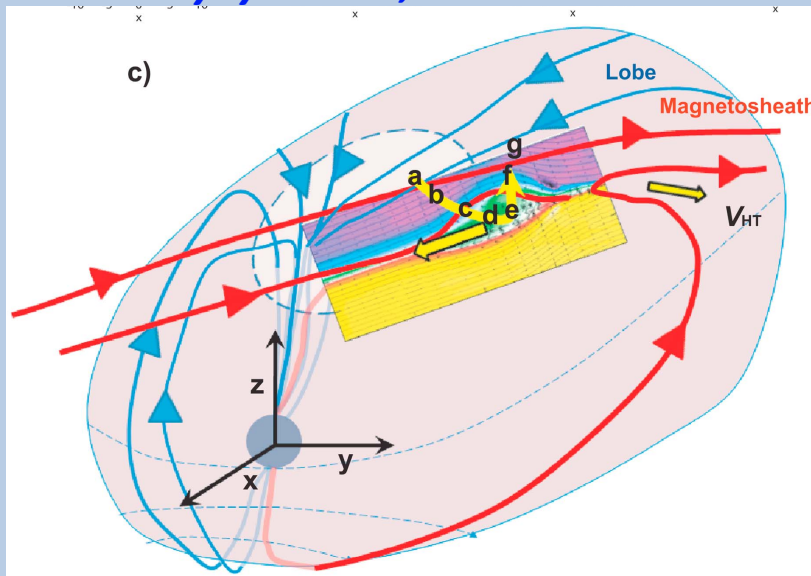
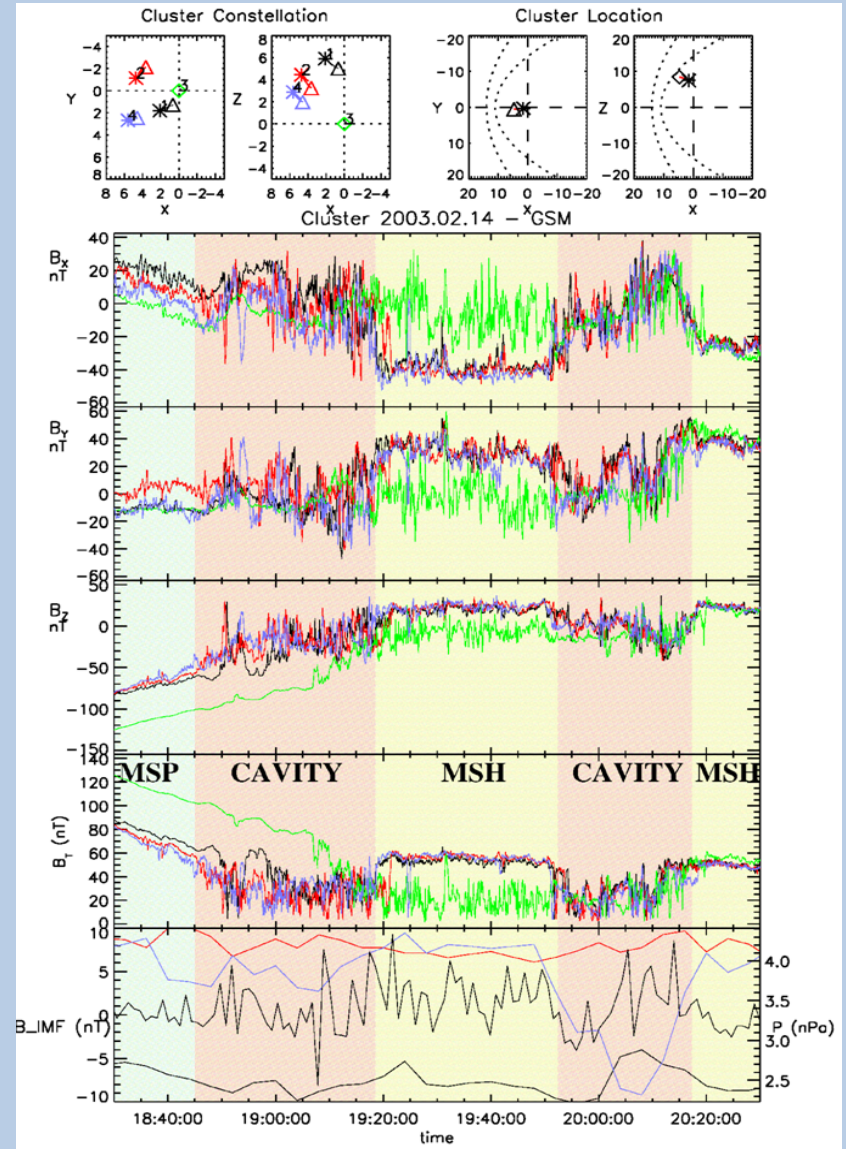


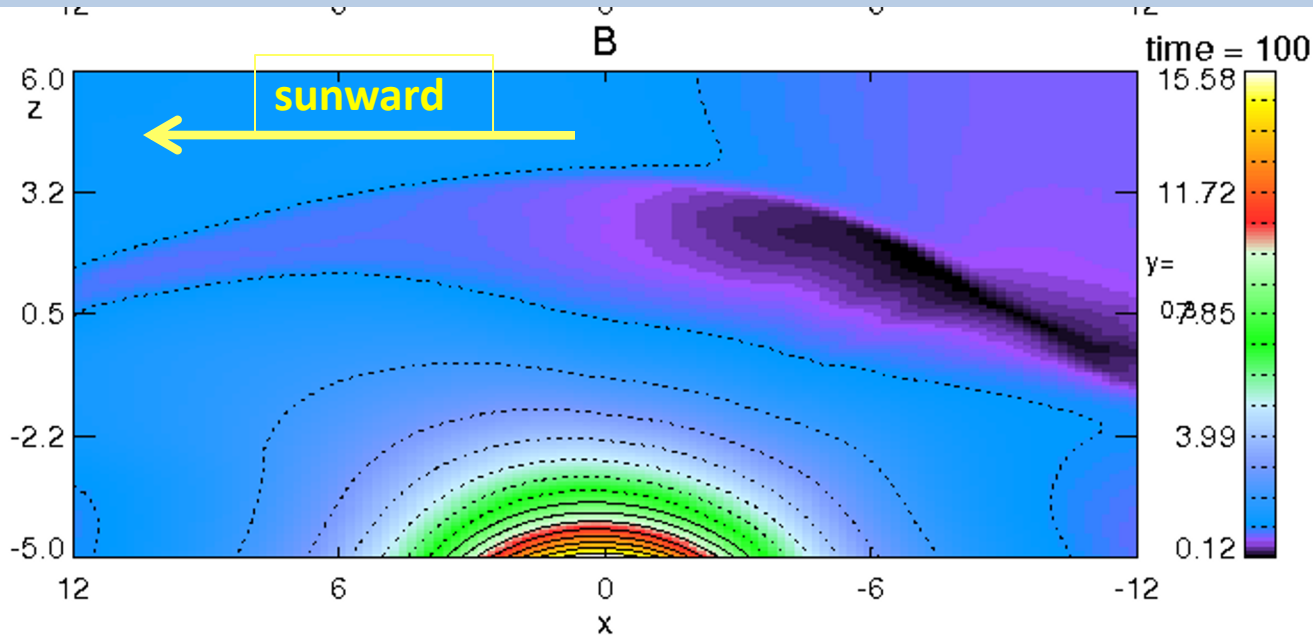
MMS virtual community workshop, April 7<sup>th</sup>, 2021

# Background: Observations of Structure of Diamagnetic Cavity in Northern hemisphere with Cluster at 5000 km separations



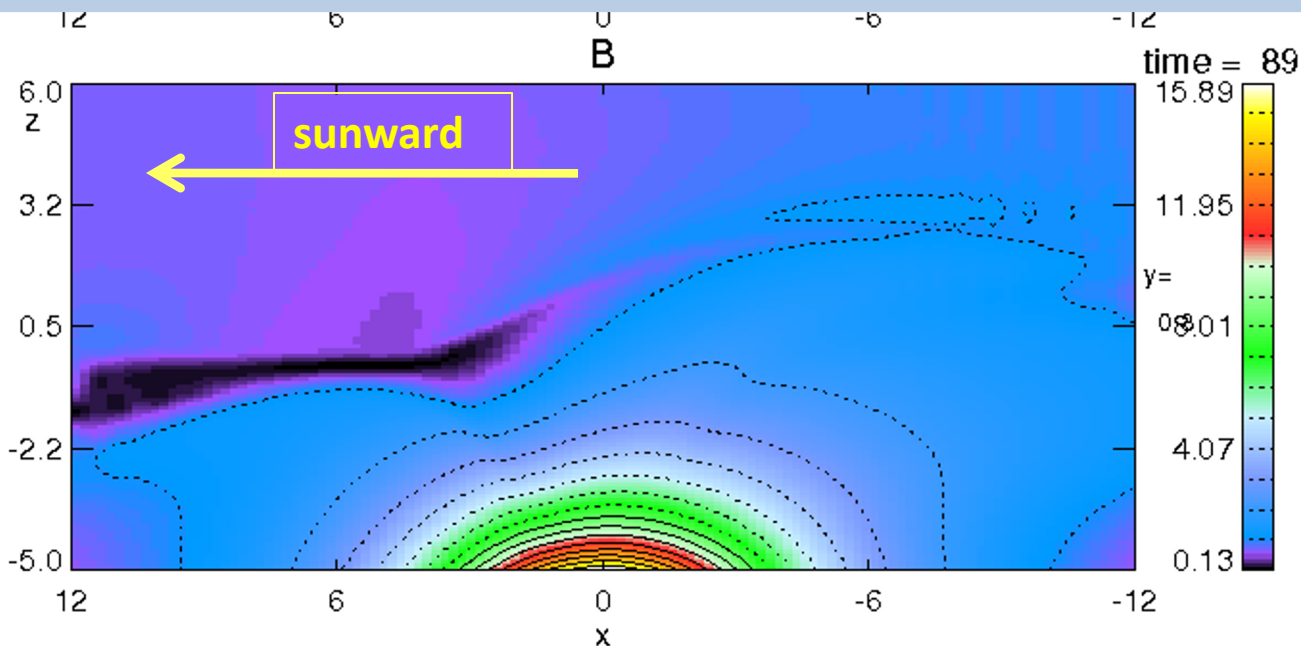
Nykyri et al., JGR 2011a





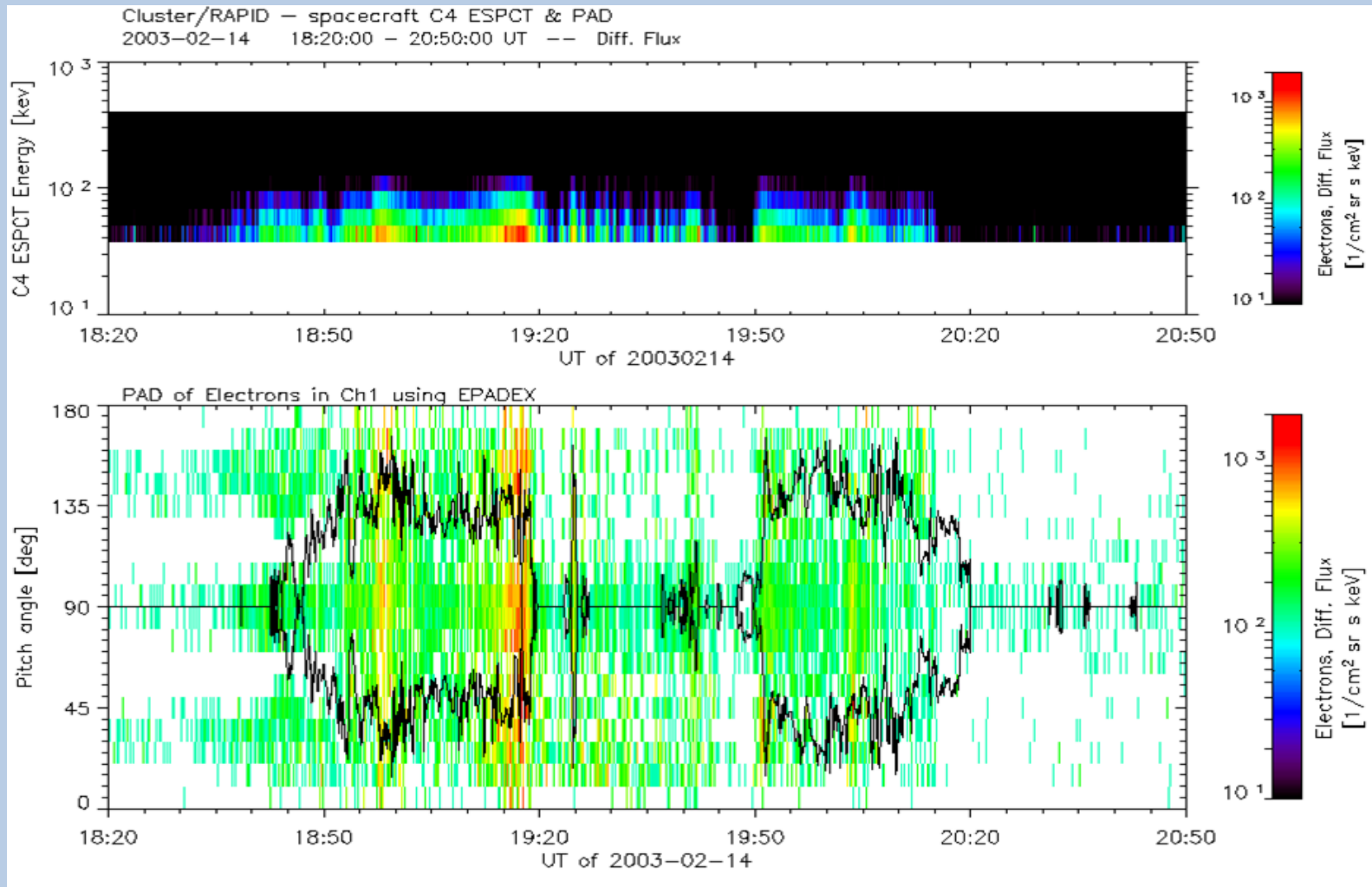
**IMF  $B_z > 0$**

- When IMF turns southward, the cavity moves sunward



**IMF  $B_z < 0$**

# Electron pitch angles and trapping condition assuming adiabatic electron motion



Nykyri et al., 2012

Trapping angle=

$$\alpha = \tan^{-1} \left( \frac{1}{\sqrt{\frac{B_{msh}}{B_{cavity}} - 1}} \right)$$

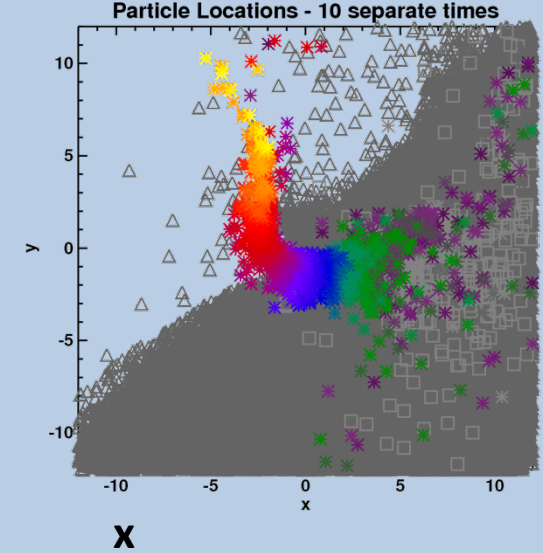
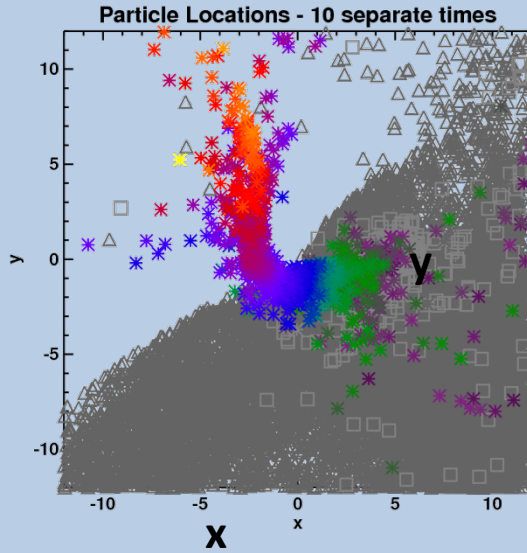
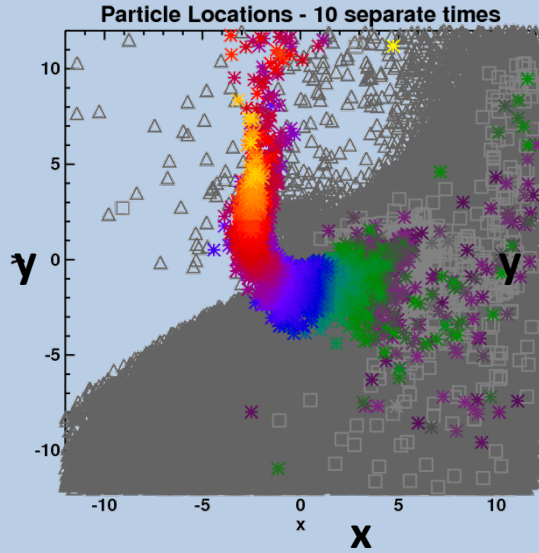
# Test Particle Simulations in 3-D High-Resolution Cusp Model

$B_0 = 40 \text{ nT}, L = 1 R_E$

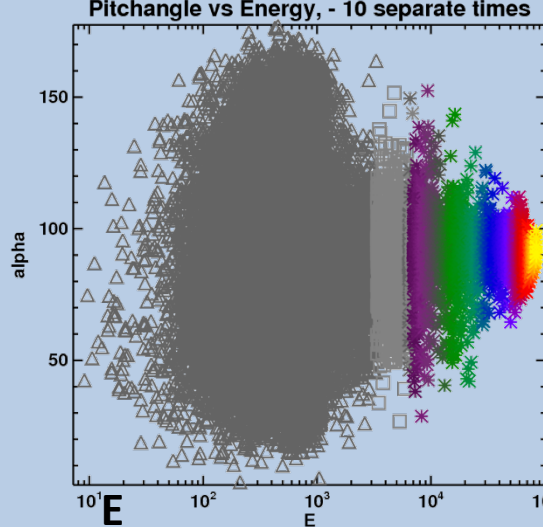
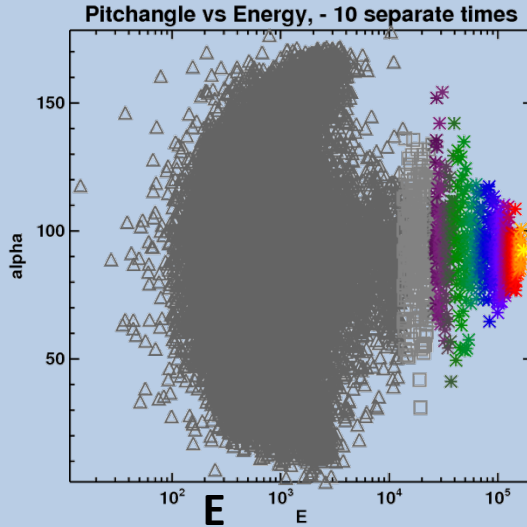
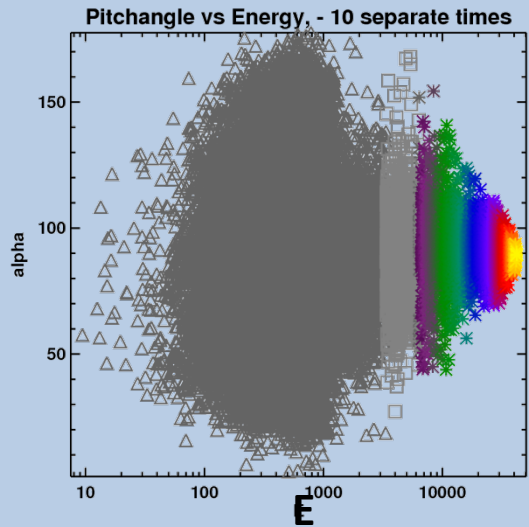
$B_0 = 80 \text{ nT}$

$L = 2 R_E$

Particle  
drift  
paths:



Particle  
Distrib:



Max. Energy:

$\sim 50 \text{ keV}$

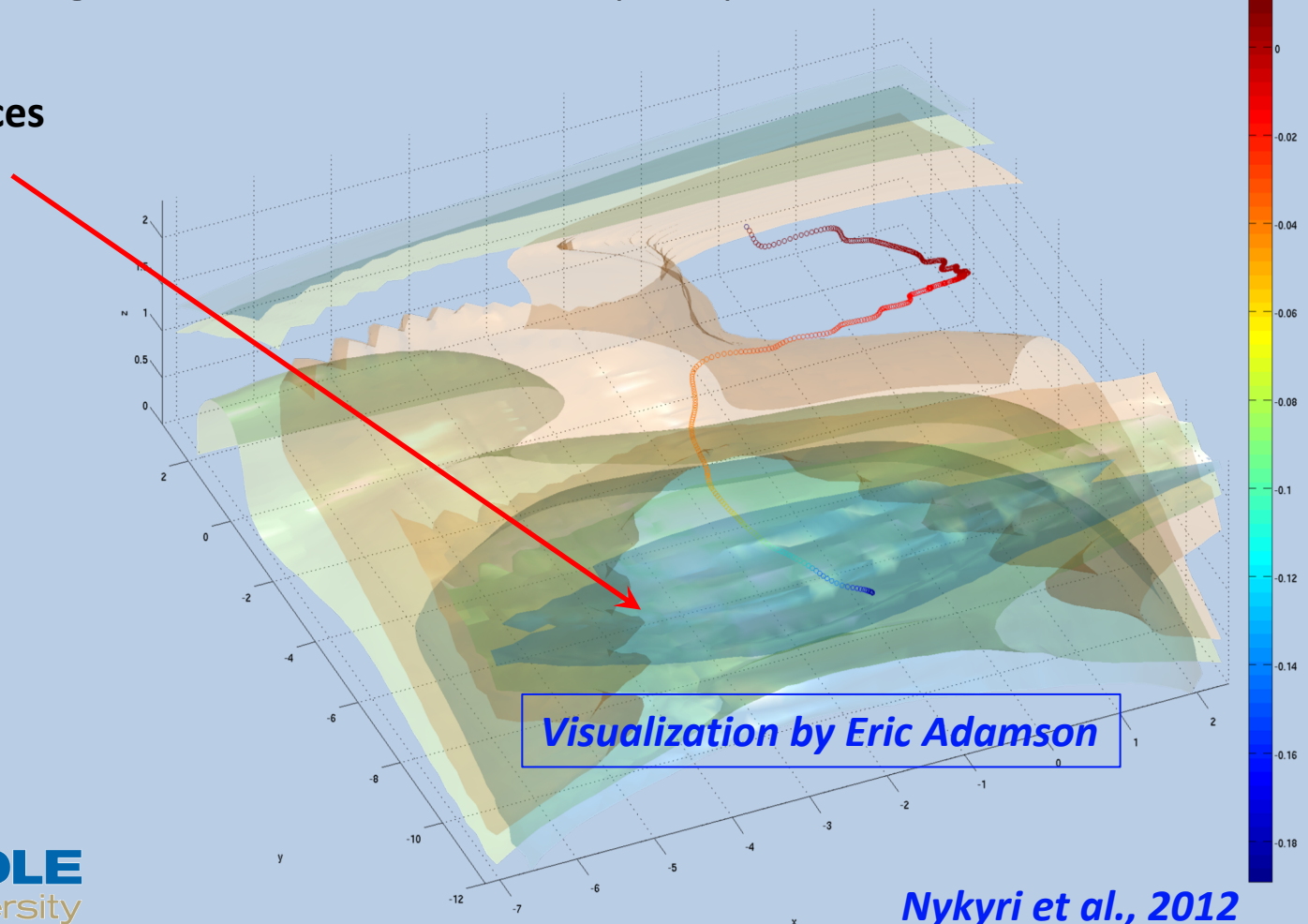
$\sim 200 \text{ keV}$

$\sim 100 \text{ keV}$

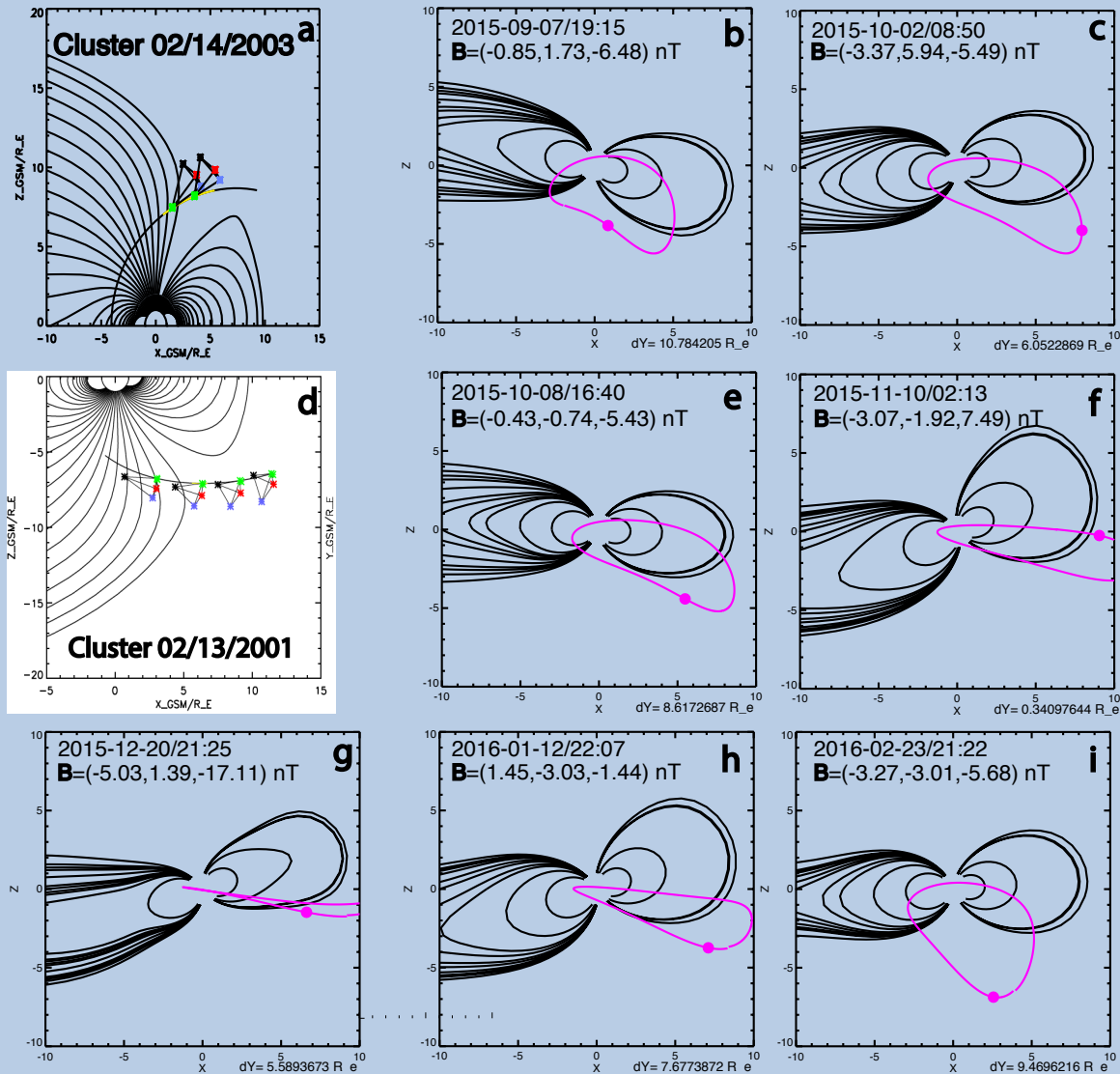
# Cusp diamagnetic cavity Acceleration Mechanism

- Particles can be accelerated in diamagnetic cavities if particle drift paths coincide with the gradients of reconnection quasi-potential.

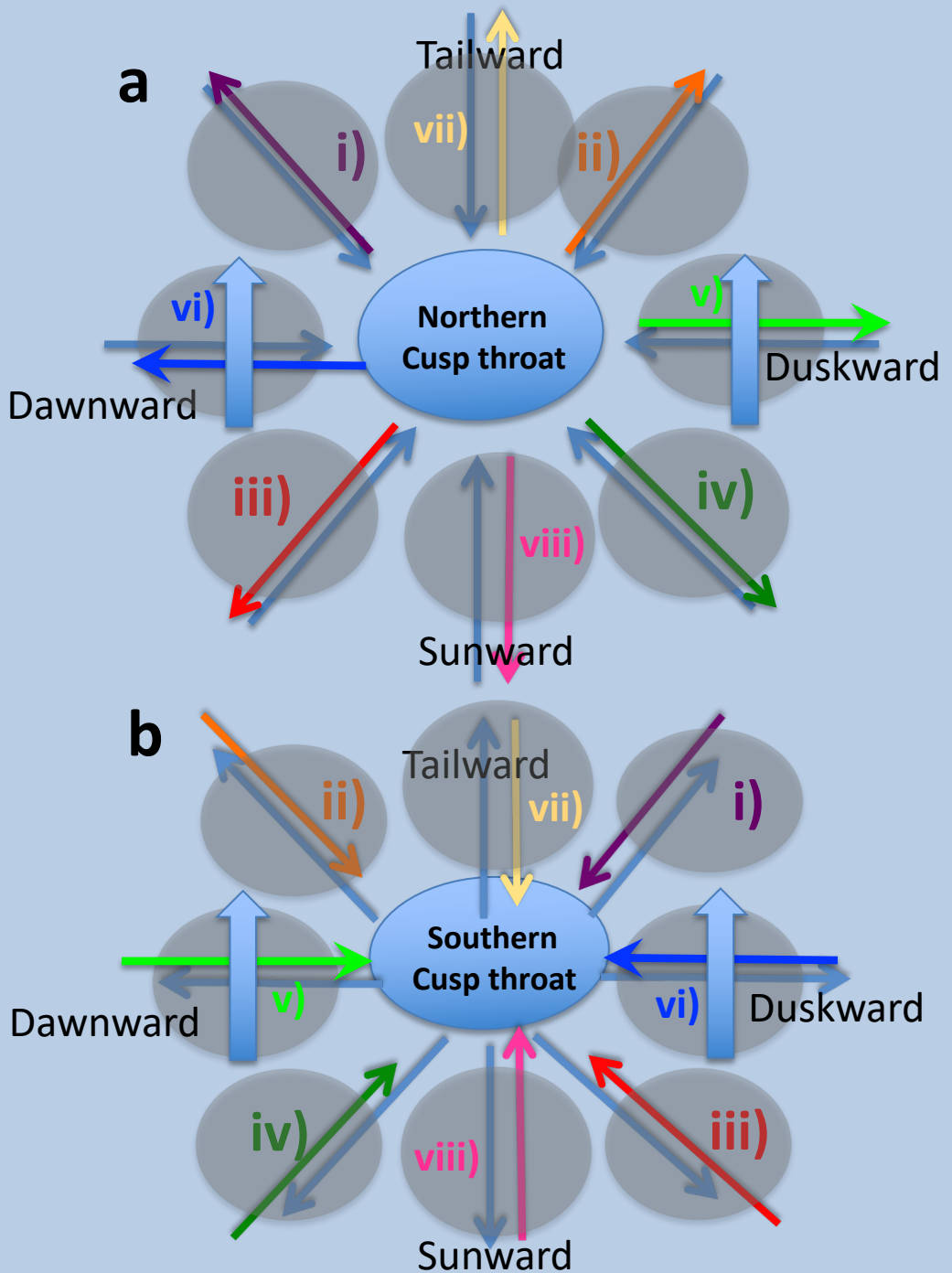
'Potential' isosurfaces



# MMS Can Reach High-Latitudes



# Cavity Formation vs. Draped IMF orientation -paradigm after Cluster

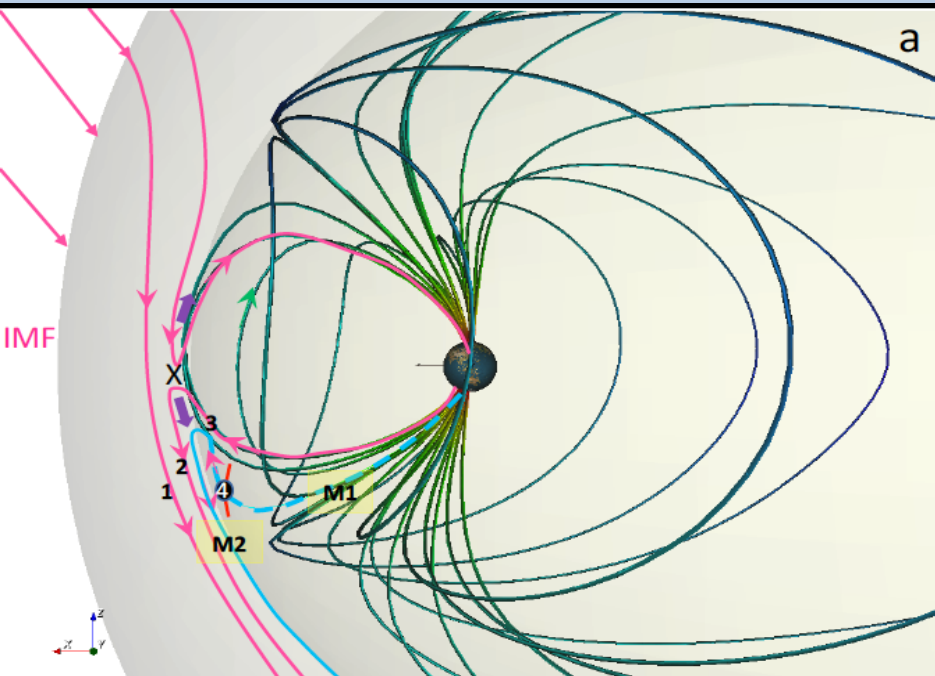


# First MMS observations of high-energy particles in a magnetic bottle in an unexpected location- a new paradigm after MMS for cavity location

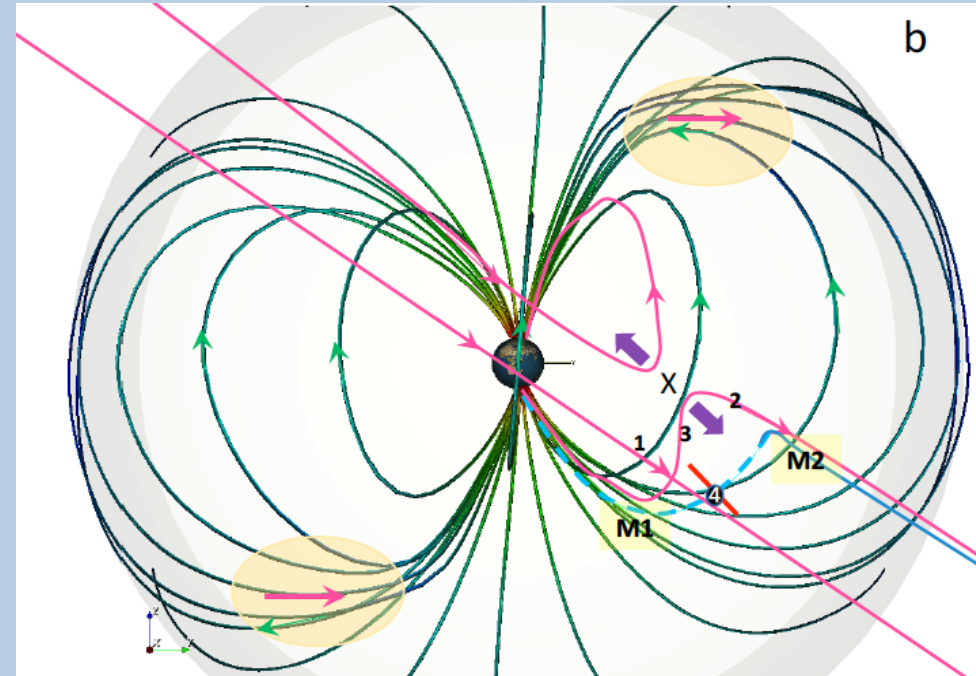
*Nykyri et al., JGR, 2019a*

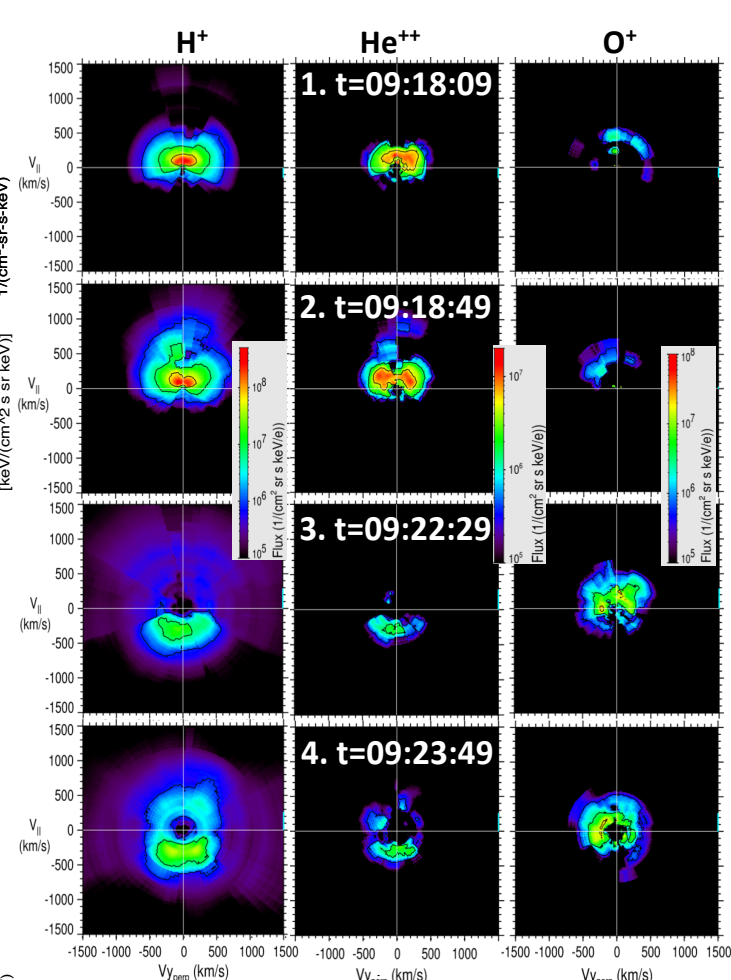
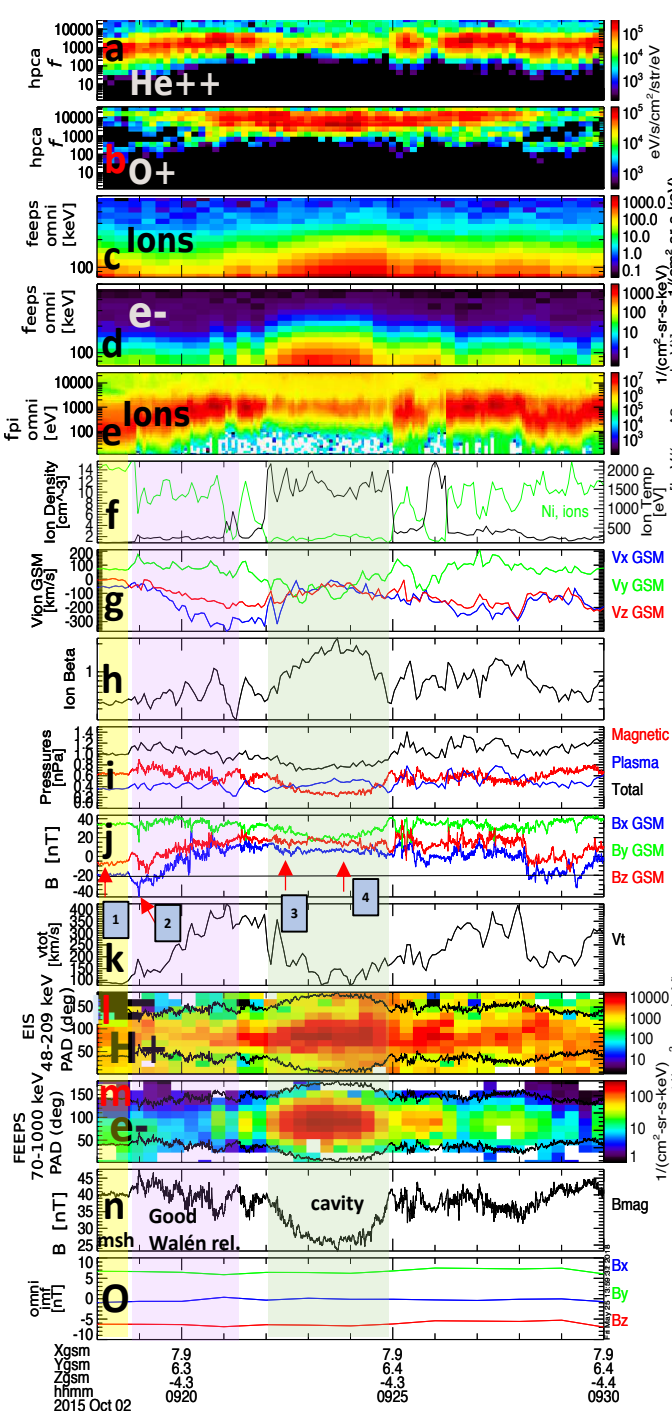
- IMF Orientation, MMS Trajectory and Magnetic field Topology from Tsyganenko 96 model

X-Z<sub>GSM</sub> -plane, view from +Y



Y-Z<sub>GSM</sub> -plane, view from +X

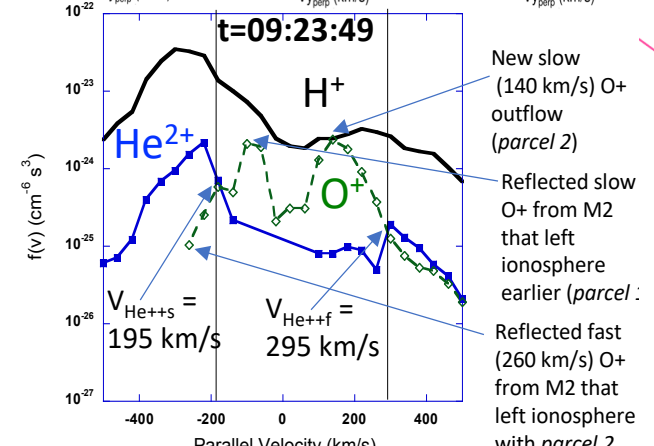




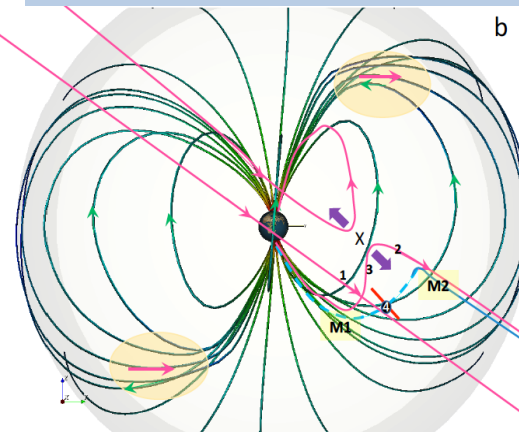
- MMS1 Observations between 9:18-9:30 during 4<sup>th</sup> cavity encounter showing presence of trapped 70keV -1MeV electrons and 48-209 keV protons as well as ~10keV O+ and He++.

- H<sup>+</sup>, He<sup>++</sup> and O<sup>+</sup> velocity distributions (MMS HPCA) reveal O<sup>+</sup> ionospheric outflow through M1 which gets reflected back at M2.

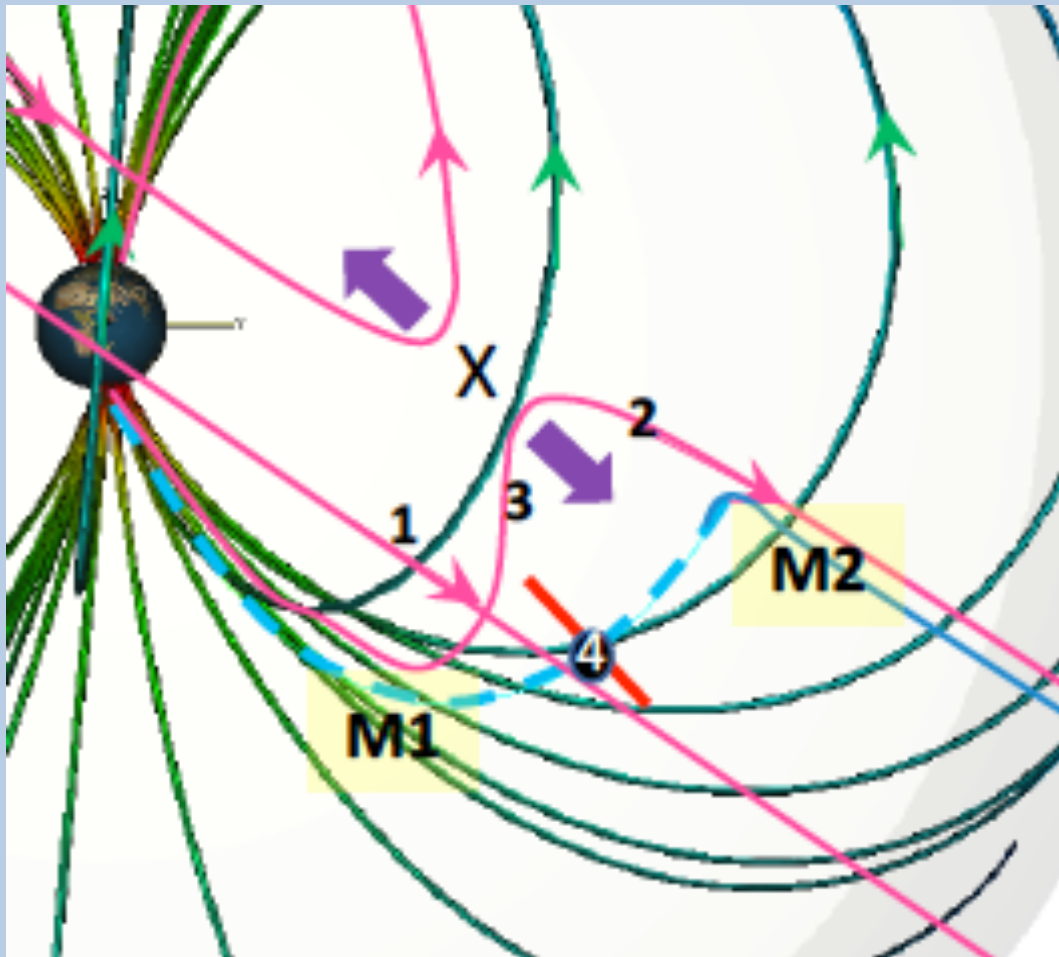
*Nykyri et al., JGR, 2019a*



- New slow (140 km/s) O<sup>+</sup> outflow (parcel 2)
- Reflected slow O<sup>+</sup> from M2 that left ionosphere earlier (parcel 1)
- Reflected fast (260 km/s) O<sup>+</sup> from M2 that left ionosphere with parcel 2



- Distance from MMS location to the reconnection site and M2 can be estimated using the fast and slow He<sup>++</sup> and O<sup>+</sup> parallel velocities observed by MMS in the cavity at t=09:23:49.



*Nykyri et al., JGR, 2019a*

$$L_{M1} = 2-2.5 R_E$$

$$V_{He^{++}t_1} = L_R + L_{M1} + L_{M1}$$

$$V_{He_s^{++}t_1} = L_R$$

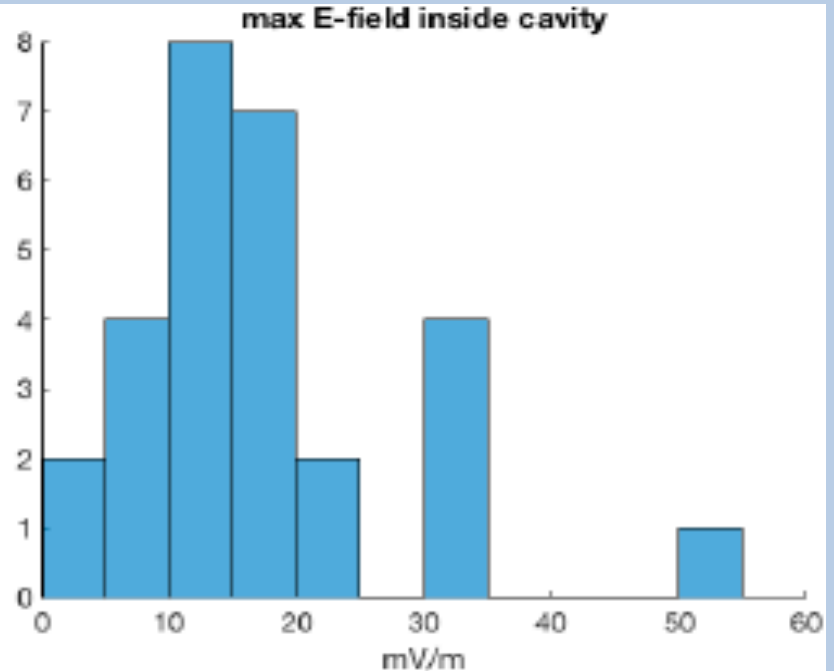
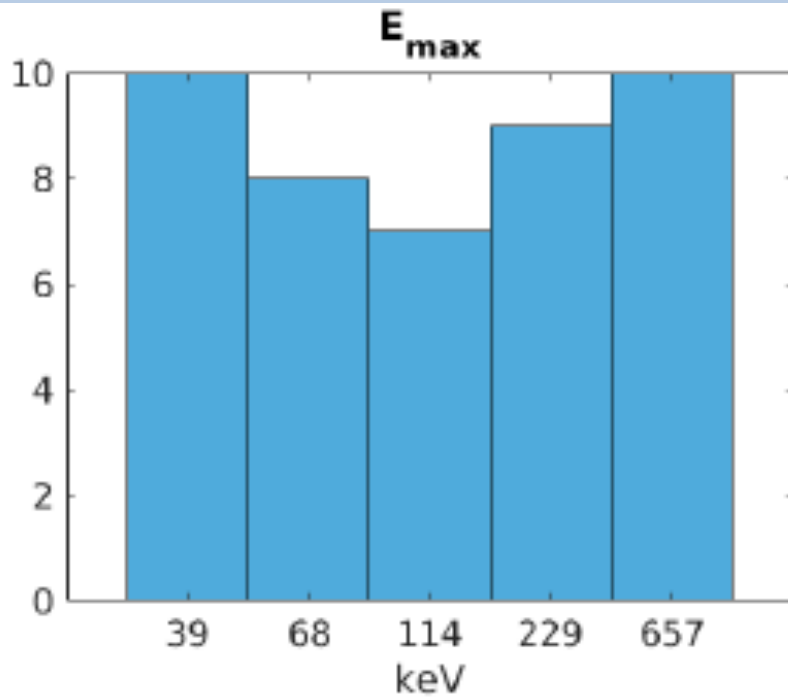
$$L_R = \frac{2V_{He_s^{++}}L_{M1}}{V_{He_f^{++}} - V_{He_s^{++}}} = 7.8 - 9.8 R_E$$

$$L_{M2} = \frac{V_{O_f^+} - V_{O_s^+}}{2V_{O_s^+}} L_{M1} = 0.9-1.1 R_E$$

# Statistics of the MMS observations of 44 diamagnetic cavities with High-Energy Electrons

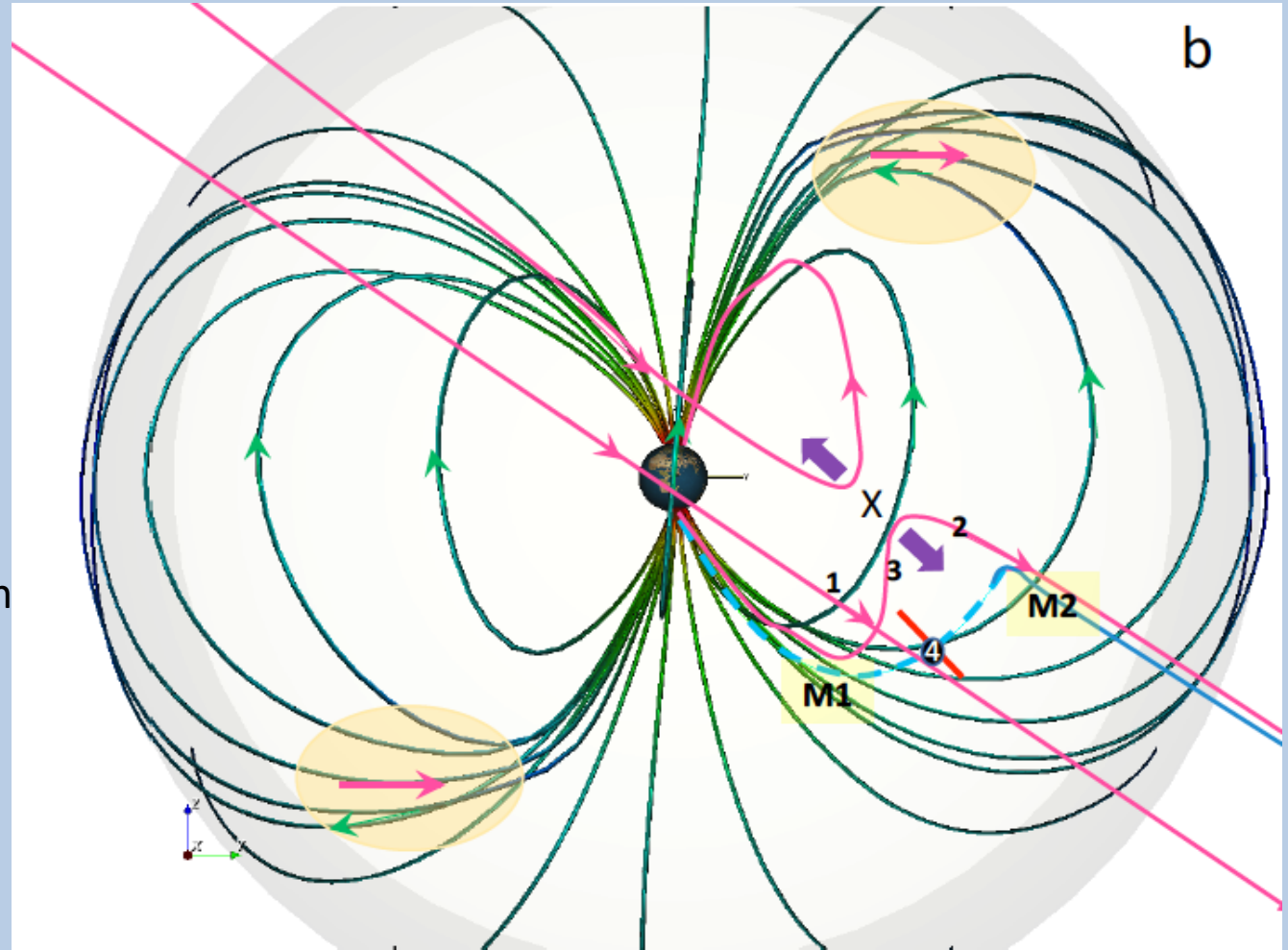
- Statistics on cavity location consistent with formation both by low- and high-latitude reconnection, and some were not consistent with either (KHI, Foreshock transients?).
- Electric fields sufficient to produce acceleration up to 100s of keV.
- Electric fields in the cavities consistent mostly with  $-\mathbf{v} \times \mathbf{B}$  electric field.

*Burkholder et al., JGR, 2020c*



# A New Paradigm for Cavity Location after Cluster and MMS

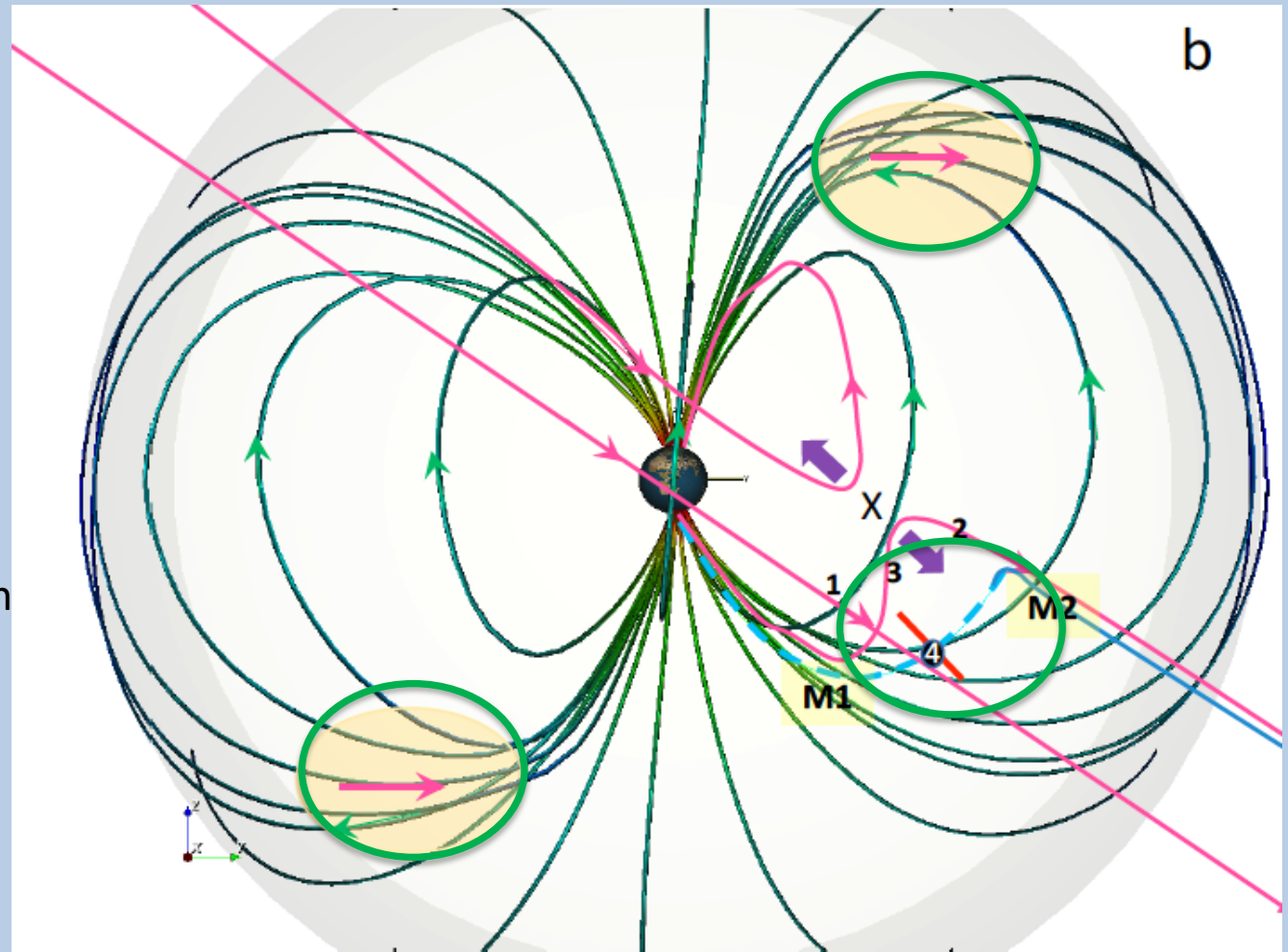
1. IMF  $B_z < 0, B_y > 0$ 
  - 3 locations
2. IMF  $B_z < 0, B_y < 0$ 
  - 3 locations
3. IMF  $B_z > 0, B_z < 0$  (dominant)
  - 2 + 2 locations
4. IMF  $B_y > 0, B_y < 0$  (dominant)
  - 2 + 2 locations
5. IMF  $B_x < 0 (B_x > 0)$  will add to draped IMF  $B_z$  Influence
6. **Hybrid IMF** for any given Dominant direction will slightly shift location Sunward, Duskward, Tailward or Dawnward



# A New Paradigm of Cavity Location

## after Cluster and MMS

1. IMF  $B_z < 0, B_y > 0$ 
  - 3 locations
2. IMF  $B_z < 0, B_y < 0$ 
  - 3 locations
3. IMF  $B_z > 0, B_z < 0$  (dominant)
  - 2 + 2 locations
4. IMF  $B_y > 0, B_y < 0$  (dominant)
  - 2 + 2 locations
5. IMF  $B_x < 0$  ( $B_x > 0$ ) will add to draped IMF  $B_z$  Influence
6. **Hybrid IMF** for any given Dominant direction will slightly shift location Sunward, Duskward, Tailward or Downward

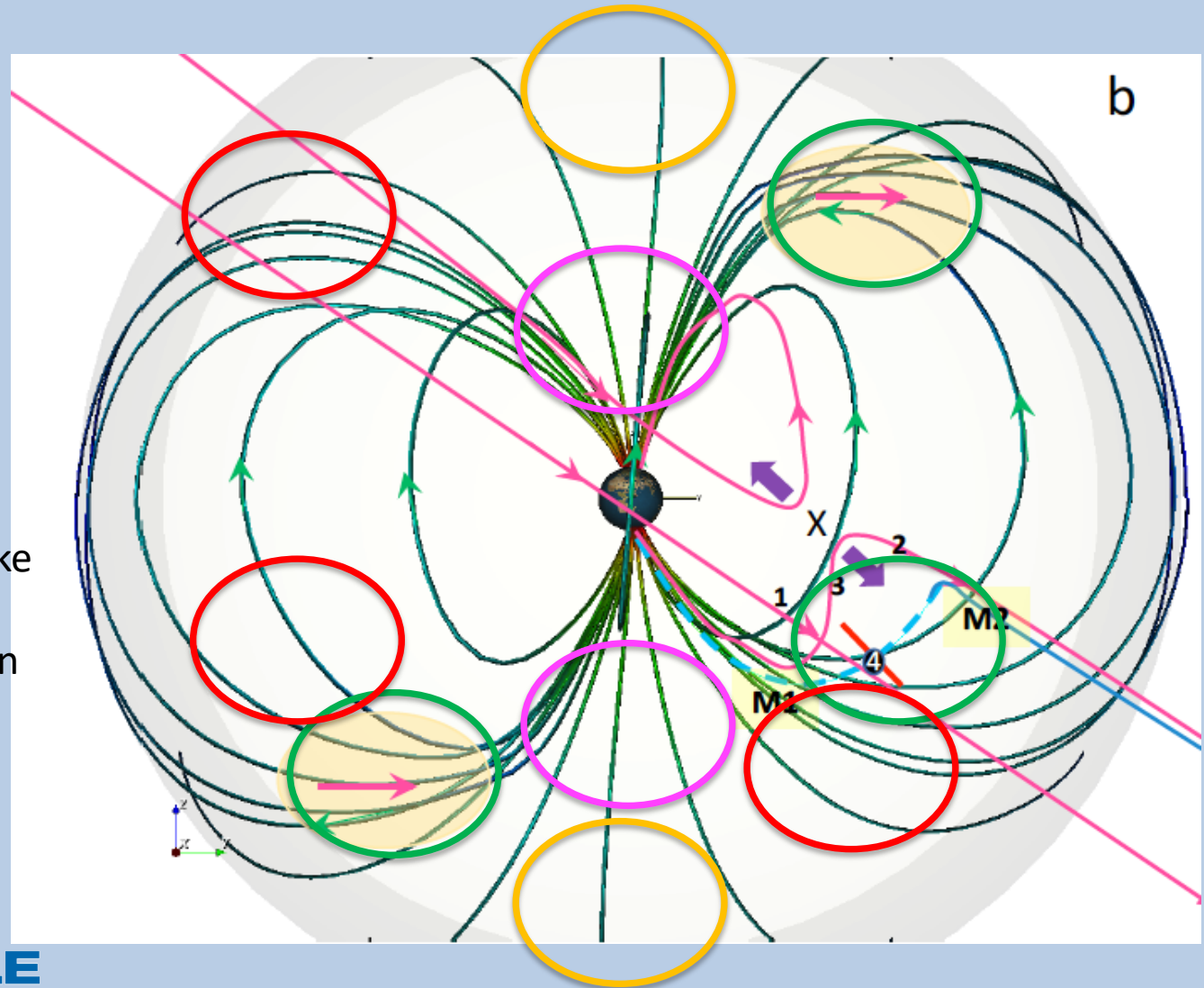




# A New Paradigm of Cavity Location

## after Cluster and MMS

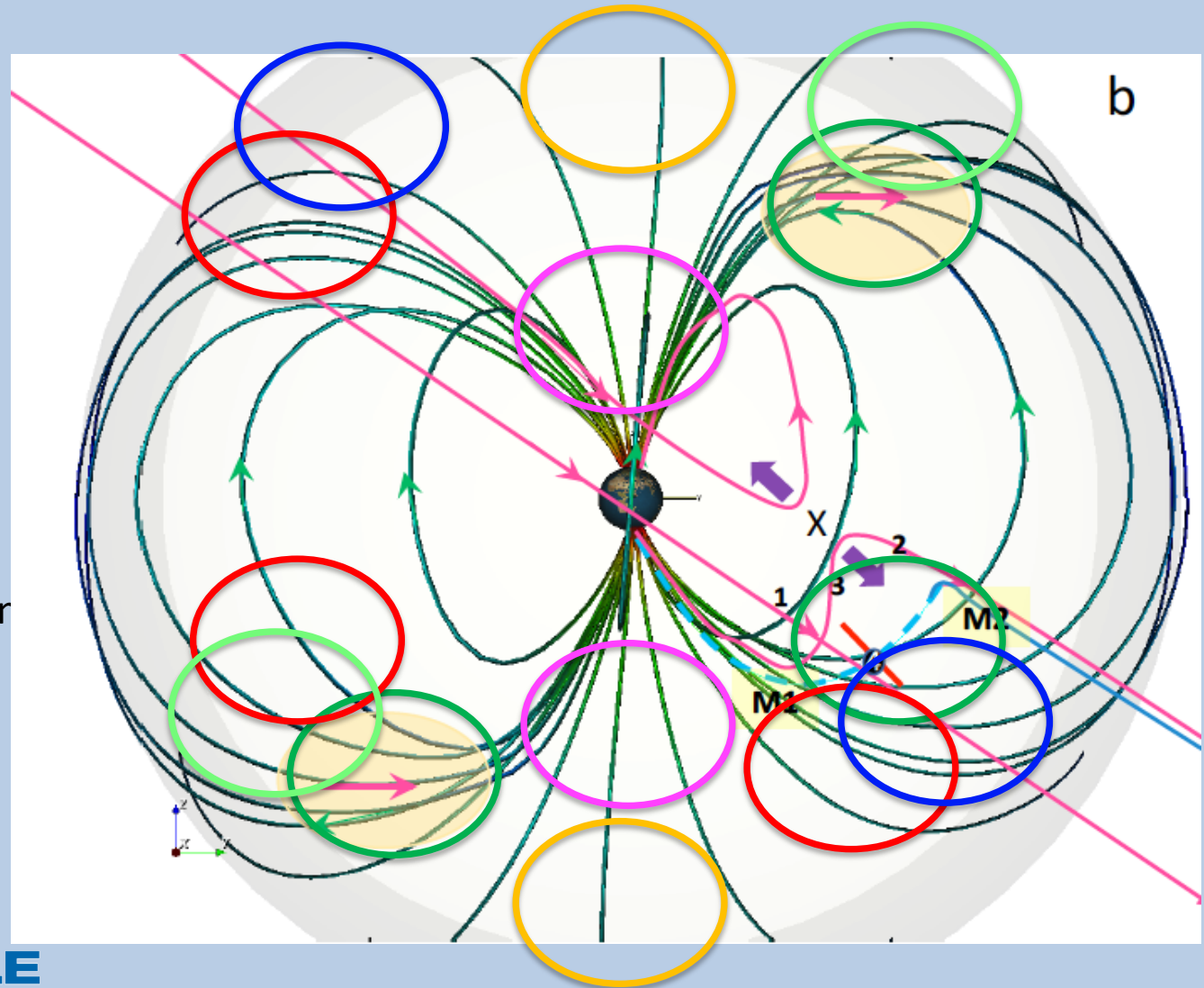
1. IMF  $B_z < 0, B_y > 0$ 
  - 3 locations
2. IMF  $B_z < 0, B_y < 0$ 
  - 3 locations
3. IMF  $B_z > 0, B_z < 0$  (dominant)
  - 2 +2 locations
4. IMF  $B_y > 0, B_y < 0$  (dominant)
  - 2+2 locations
5. IMF  $B_x < 0 (B_x > 0)$  will add to draped IMF  $B_z$  Influence ( $B_x < 0$ , will act like  $B_z < 0$  and vice versa)
6. Hybrid IMF for any given Dominant direction will slightly shift location Sunward, Duskward, Tailward or Dawnward



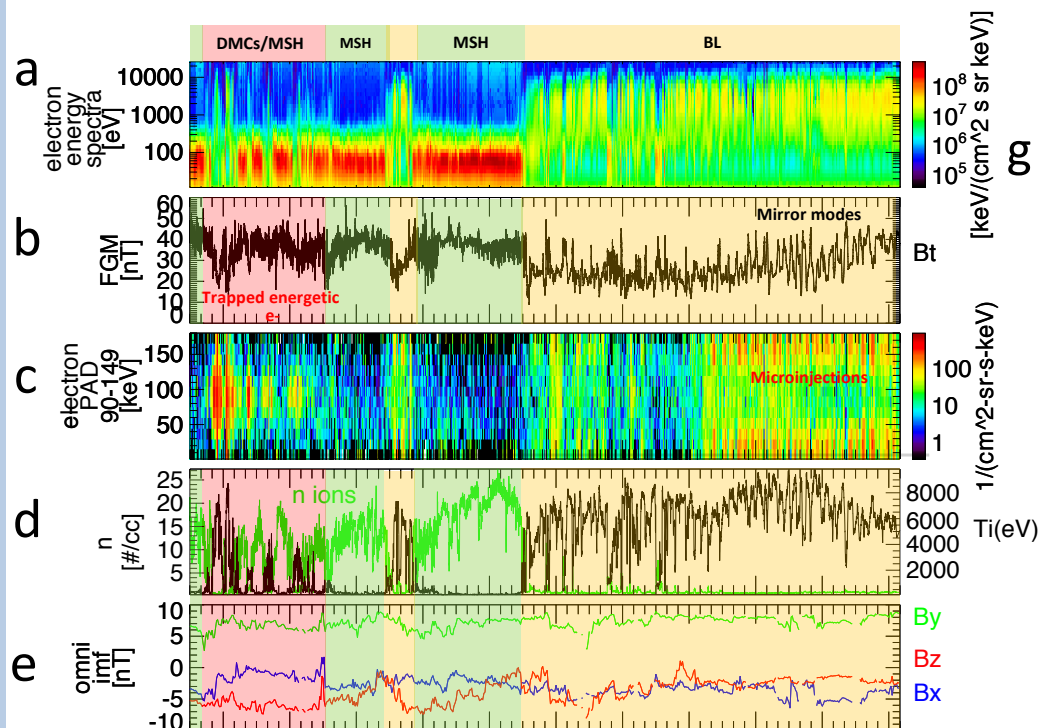
# A New Paradigm of Cavity Location

## after Cluster and MMS

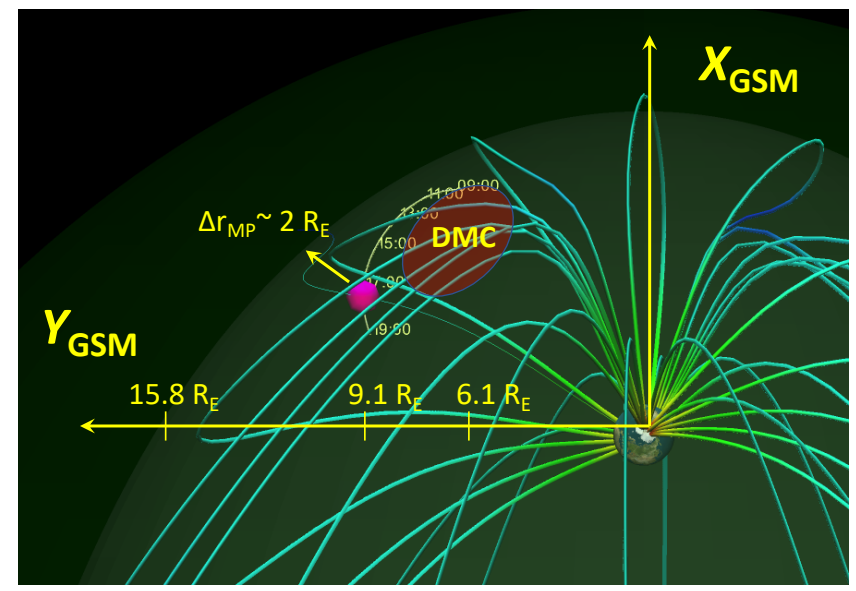
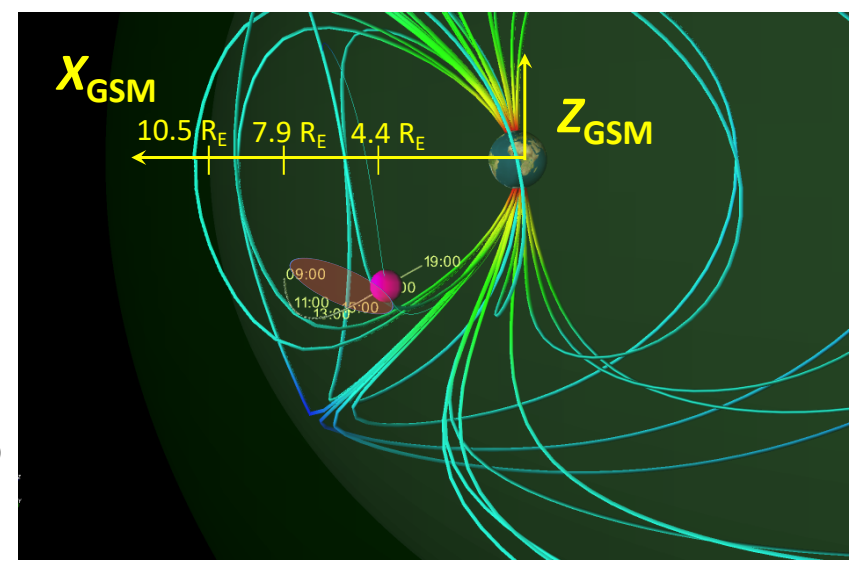
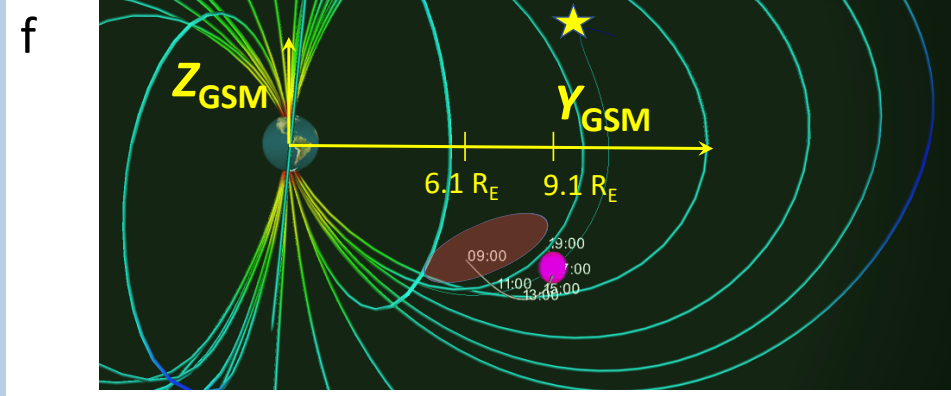
1. IMF  $B_z < 0, B_y > 0$ 
  - 3 locations
2. IMF  $B_z < 0, B_y < 0$ 
  - 3 locations
3. IMF  $B_z > 0, B_z < 0$   
(dominant)
  - 2 + 2 locations
4. IMF  $B_y > 0, B_y < 0$   
(dominant)
  - 2 + 2 locations
5. IMF  $B_x < 0 (B_x > 0)$   
will add to draped IMF  $B_z$   
Influence
6. **Hybrid IMF** for any given  
Dominant direction will  
slightly shift location  
Sunward, Duskward, Tail-  
ward or Dawnward







MLT	14.7	14.8	14.9	15.1	15.2	15.4	15.6	15.8	16.0	16.3	16.6
r	10.8	11.3	11.6	11.9	12.0	12.0	11.9	11.6	11.3	10.8	10.2
Xgsm	7.9	7.9	7.7	7.4	7.0	6.6	6.0	5.4	4.8	4.0	3.2
Ygsm	6.1	6.7	7.2	7.6	8.0	8.4	8.8	9.0	9.1	9.1	8.9
Zgsm	-4.1	-4.6	-5.1	-5.3	-5.4	-5.4	-5.2	-4.9	-4.5	-4.1	-3.6
hhmm	0900	1000	1100	1200	1300	1400	1500	1600	1700	1800	1900



# Particles from the diamagnetic cavities can be the source for the energetic electron microinjections.

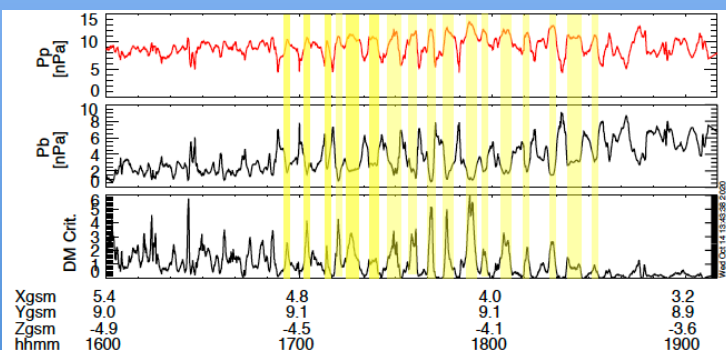
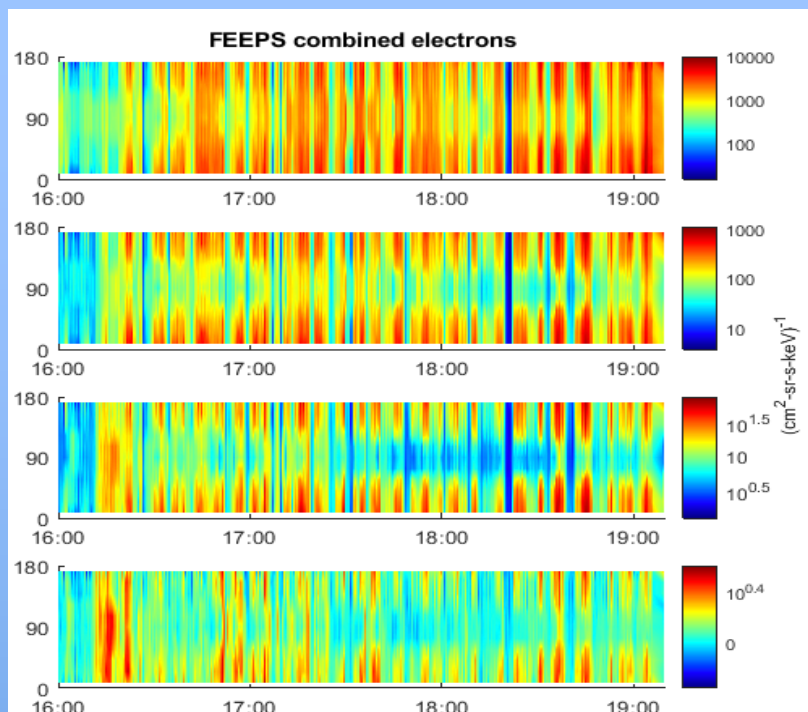
## Electron PADs

40-70 keV

70-130 keV

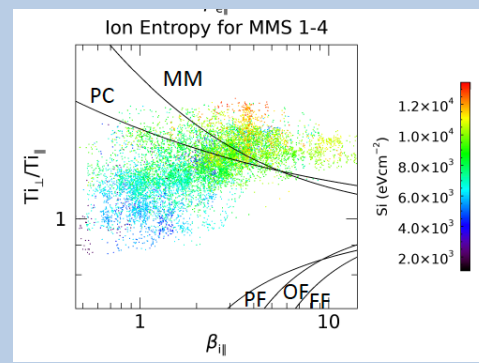
130-250 keV

250-550 keV



*Nykyri et al., 2021b, submitted*

- MMS observed for  $\sim 3$  hrs 28-550 keV electron microinjections in the high-latitude magnetosphere 4  $R_E$  away from the diamagnetic cavities.
- Dispersionless nature  $\rightarrow$  MMS near the source source region.
- Acceleration mechanism  
In cavity creates Ion temperature anisotropy  
 $\rightarrow$  Drift mirror instability



# Mass content in the cavities for any given IMF orientation

IMF  $B_y > 0$   
 IMF  $B_z > 0$   
 IMF  $B_z < 0$

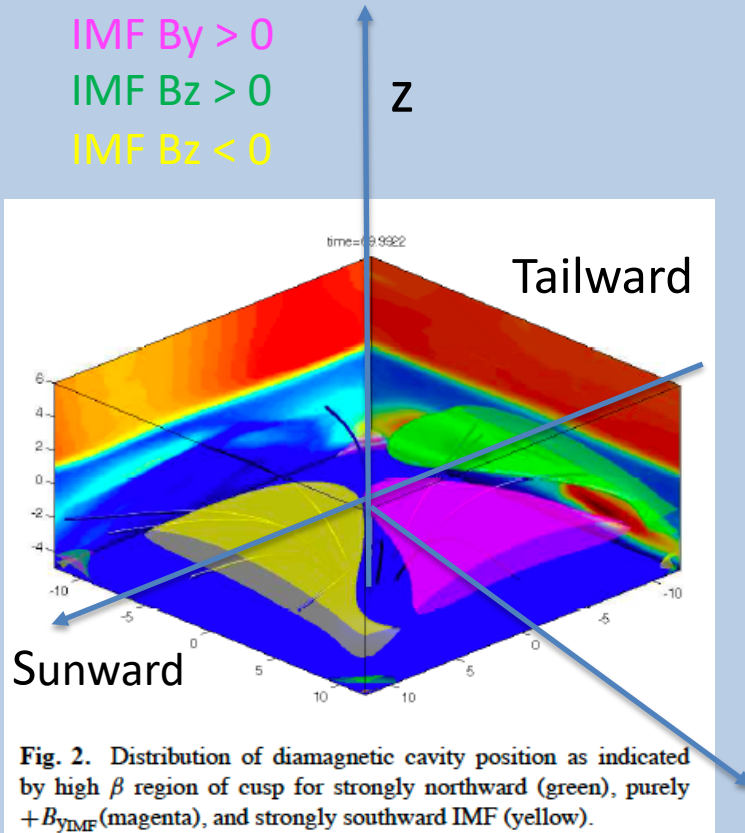


Fig. 2. Distribution of diamagnetic cavity position as indicated by high  $\beta$  region of cusp for strongly northward (green), purely  $+B_{yIMF}$  (magenta), and strongly southward IMF (yellow).

Adamson et al., *Angeo*, 2012

Lower energy particles (Cluster CIS fluxes about  $10^7 \# / (\text{cm}^2 \text{sr s keV})$ ):

Mass of the plasma in a typical cavity created by high-latitude reconnection

$M = nmV \sim (15 \times 12 \times 2 / 2) R^3 = 10e6 / \text{m}^3 * 1.67e-27 \text{ kg} * 4.6531e22$   
 $M = 777 \text{ kg}$  (assuming protons)  
 North+South  $\rightarrow M = 2 \times 777 \text{ kg} = \underline{1554 \text{ kg}}$

Mass of the plasma in a typical cavity created by low-latitude reconnection

$M = nmV \sim (7.5 \times 12 \times 4 / 2) R^3 = 2e6 / \text{m}^3 * 1.67e-27 \text{ kg} * 4.6531e22$   
 $M = 155 \text{ kg}$  (assuming protons)  
 South only.

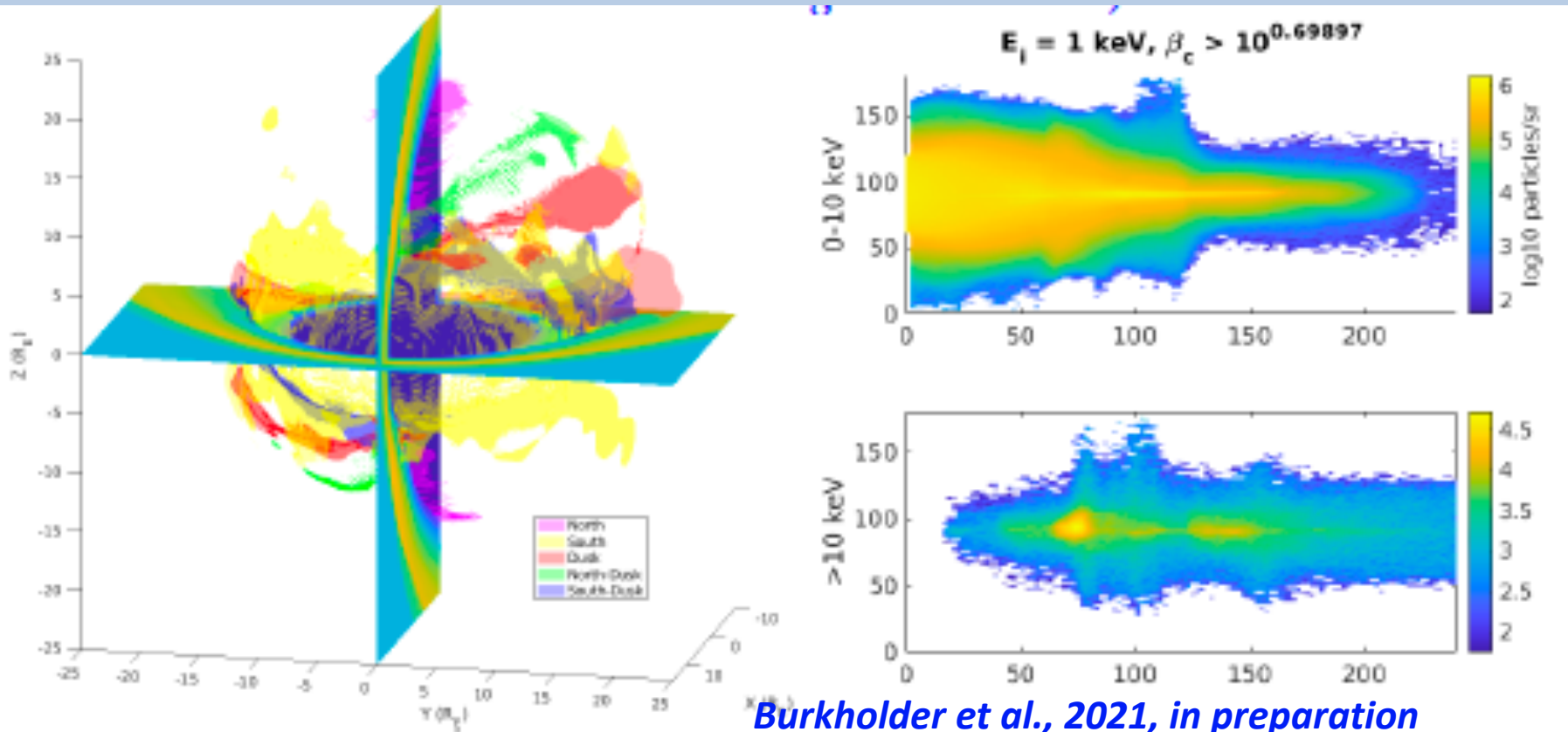
So for  $B_z < 0$  with  $B_y > 0$  or  $B_z < 0$ , the total proton **mass in cavities**  $1554 \text{ kg} + 155 \text{ kg} \sim \underline{1710 \text{ kg}}$ .

Assuming typical plasma sheet density  $n$  during southward IMF of  $0.5 / \text{cc}$ , this volume would correspond to mass of only 38 kg.

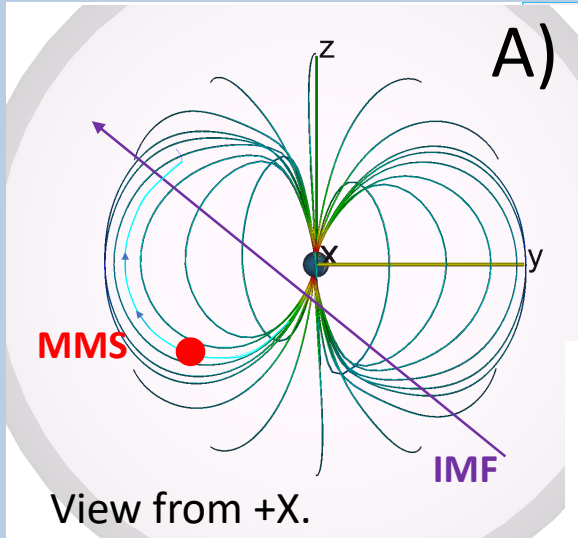
The 40-70 keV proton and electron fluxes during dayside microinjections are  $10^5 \# / (\text{cm}^2 \text{sr s keV})$ .

# GAMERA global simulations of the cavity formation and particle energization

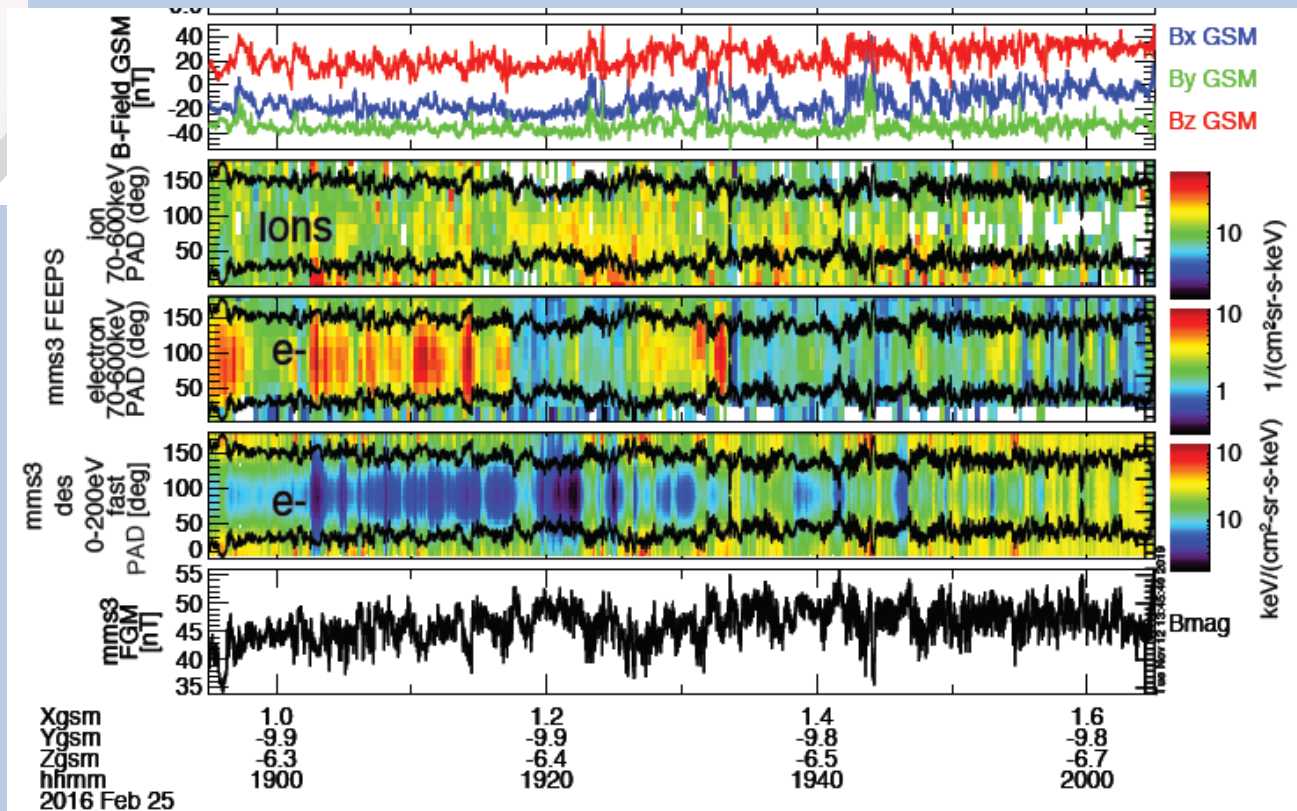
- Cavity acceleration energizes particles perpendicular to magnetic field  
⇒ Possible source for temperature anisotropy and high-plasma beta in high-latitude magnetosphere capable for drive the drift mirror instability.



# Open questions: Interaction between KH waves, mirror-mode waves and diamagnetic cavities at high-latitudes?



- New MMS orbits at high-altitude cusp with *string-of-pearls* separation with 2 spacecraft about 1000-2000 km apart and few in 100-200 km separations (together with TRACERS at low Altitudes and HSO fleet) would be ideal studying these processes



Nykyri et al., JGR, 2021a

# Conclusions

- Large, several  $R_E$  in size, diamagnetic cavities can be generated at high-latitudes by high-and low-latitude reconnection. Particles can gain several 100s of keV if cavity remains stable for 4-5 minutes.
- For any given IMF orientation, at least 2 cavities form, one at northern and one at southern hemispheric, high-latitude magnetosphere.
- For  $B_z < 0$ ,  $B_y > 0$  and for  $B_z < 0$ ,  $B_y < 0$  we get additional cavities at southern hemisphere due to low latitude component reconnection.
- Mass in the cavities for  $B_z < 0$ ,  $B_y > 0$  and for  $B_z < 0$ ,  $B_y < 0$  is comparable to mass in near-earth magnetotail.
- The particles are accelerated in the cavities perpendicular to magnetic field which could explain the origin of strong temperature anisotropy, high plasma beta and make conditions ripe for drift mirror instability, which can drive energetic electron microinjections.
- These particles may gain access to inner magnetosphere and could contribute to radiation belt seed population.